Advances in Nano Research, *Vol. 16, No. 2 (2024) 187-200*
https://doi.org/10.12989/anr.2024.16.2.187

Small-scale effects on wave propagation in curved nanobeams subjected to thermal loadings based on NSGT

Ibrahim Ghoytasi*[1] and Reza Naghdabadi[1,2]

[1]*Department of Mechanical Engineering, Sharif University of Technology, Tehran 1458889694, Iran*
[2]*Institute for Nanoscience and Nanotechnology, Sharif University of Technology, Tehran 1458889694, Iran*

(*Received March 26, 2023, Revised August 27, 2023, Accepted December 14, 2023*)

Abstract. This study focuses on wave propagation analysis in the curved nanobeam exposed to different thermal loadings based on the Nonlocal Strain Gradient Theory (NSGT). Mechanical properties of the constitutive materials are assumed to be temperature-dependent and functionally graded. For modeling, the governing equations are derived using Hamilton's principle. Using the proposed model, the effects of small-scale, geometrical, and thermo-mechanical parameters on the dynamic behavior of the curved nanobeam are studied. A small-scale parameter, Z, is taken into account that collectively represents the strain gradient and the nonlocal parameters. When $Z<1$ or $Z>1$, the phase velocity decreases/increases, and the stiffness-softening/hardening phenomenon occurs in the curved nanobeam. Accordingly, the phase velocity depends more on the strain gradient parameter rather than the nonlocal parameter. As the arc angle increases, more variations in the phase velocity emerge in small wavenumbers. Furthermore, an increase of ΔT causes a decrease in the phase velocity, mostly in the case of uniform temperature rise rather than heat conduction. For verification, the results are compared with those available for the straight nanobeam in the previous studies. It is believed that the findings will be helpful for different applications of curved nanostructures used in nano-devices.

Keywords: curved nanobeam; NSGT; small-scale effects; thermal effects; wave propagation

1. Introduction

The development of small-scale manufacturing technologies, and the advancement in material science, have paved the way for material production with desired structural features at micro- and nano-scales. Experimental reports have shown the importance of size effects on the mechanical behavior of small-scale structures (Miller and Shenoy 2000, Xu *et al.* 2010). Classical theories cannot predict variations at the nanometer level and capture the size effects on the mechanical behavior of materials (Yan and Jiang 2011). Therefore, higher-order theories have been developed to investigate mechanical behavior depending on the small-scale effects. Based on the (Mindlin 1965) strain gradient theory, (Lam *et al.* 2003) developed the Modified Strain Gradient Theory (MSGT), which incorporates three longitudinal scale parameters to capture the size effects. Then, (Yang *et al.* 2002) introduced a particular case of MSGT, called Modified Couple Stress Theory (MCST), which includes only one longitudinal scale parameter. Many studies have utilized these theories to investigate the static and dynamic behavior of microstructures (Sadeghi *et al.* 2012, Rahmani *et al.* 2017, Hu *et al.* 2018, Rahmani *et al.* 2018, Alwabli *et al.* 2021, Ghandourah *et al.* 2021).

(Eringen 1983) proposed the Nonlocal Theory (NT). In this theory, he defined stress at one point of a continuous matter as a function of strain at all points. Based on the concept of the NT, researchers have investigated the mechanical behavior of nanostructures (Eltaher *et al.* 2016, Ganapathi and Polit 2018, Barretta *et al.* 2019, Numanoğlu and Civalek 2019, Ebrahimi *et al.* 2019a, Matouk *et al.* 2020, Hadji and Avcar 2021, Wang *et al.* 2023). The MSGT only applies the local high-order strain gradients, while the NT accounts for the nonlocal effects. In order to incorporate two different small-scale effects on the size-dependent mechanical behavior, (Lim *et al.* 2015) recently introduced the Nonlocal Strain Gradient Theory (NSGT), integrating SGT and NT. They showed that this theory could predict well the stiffness-hardening effects, considering nonlocal strain gradients. Many studies have been conducted to investigate the mechanical behavior of nano-scale structures based on the NSGT (Li *et al.* 2015, 2022, Bensaid *et al.* 2018, Şimşek 2019, Alazwari *et al.* 2022, Xing *et al.* 2022). Based on the NSGT, (Li *et al.* 2015) presented an analytical model to investigate the wave propagation in FG nanobeams. They showed that, depending on the nonlocal parameter value, the phase velocity of the material could increase or decrease in general.

In recent decades, the emergence of functionally graded materials (FGMs) as novel types of composites has influenced different engineering and technology fields. Generally, the FGMs are made of two materials, for instance, metal and ceramic. The metal phase of FG materials maintains toughness. Also, due to the small thermal conductivity of the ceramic phase, these materials exhibit excellent thermal resistance (Komijani *et al.* 2013, Tlidji *et al.* 2022). Besides, the special properties of FG materials improve the stress distribution, increase the

*Corresponding author, M.Sc.,
E-mail: ibrahim.ghoytasi@alum.sharif.edu;
i.ghoytasi@gmail.com

ISSN: 2287-237X (Print), 2287-2388 (Online)

thermal resistance, as well as reduce the stress concentration, and thermal and residual stresses (Kiani 2016, Attia 2017). In addition, the high strength/stiffness to weight ratio as one of the special features of curved nanostructures has caused the widespread use of these types of structures in the field of civil and mechanical designs, as well as biotechnology and medicine (Zenkour and Sobhy 2015, Hashemian and Hosseini 2019). Accordingly, FG curved structures have been extensively used in various engineering research (Akgöz and Civalek 2013) including biomechanics (Rahaeifard *et al.* 2010), optoelectronics, high-temperature technologies, nanotechnologies, and nano-devices such as MEMS/NEMS devices (Gorgani *et al.* 2019, Zhao and Yu 2021), biosensors (Shabana *et al.* 2021), and actuators (Carbonari *et al.* 2009, Ghayesh and Farajpour 2019). The inherent characteristics of these materials make them versatile and desirable for small-scale systems and smart structures.

The Euler-Bernoulli beam Model (EBM) estimates the behavior of beams to be stiffer, neglecting the shear deformation effects. This assumption makes this model suitable for tall and narrow beams. Since shear deformations in the behavior of thick beams are prominent, the effects of this parameter are considered in the Timoshenko beam Model (TBM) (Timoshenko 1922). Many researchers have used these models to study the static and dynamic behavior of micro and nanoscale beams and plates. Papargyri-Beskou *et al.* (2009) studied the analytical wave propagation in gradient elastic solids and structures using the EBM and the Kirchhoff plate model. They showed that wave dispersion would be physically observed when both the micro-elastic and micro-inertial effects were considered in the model. Nanda and Kapuria (2015) investigated the wave propagation in laminated composite curved beams based on first-order shear deformation theory (FSDT) and classical laminate theory (CLT). They demonstrated a significant difference between the results predicted by the CLT and FSDT and revealed that CLT is inefficient for wave propagation analysis. Based on the NSGT, Li *et al*. (2015) presented an analytical model to investigate wave propagation in FG nanobeams. They showed that, in general, depending on the nonlocal parameter value, the phase velocity of the material can be increased or decreased. Mohammadimehr *et al*. (2016) studied the vibration and wave propagation of a twisted microbeam based on the SGT. They indicated that increasing the rate of twist angle leads to an increase in the phase velocity.

Arefi and Zenkour (2017) analyzed the wave propagation of the Timoshenko FG magneto-electro-elastic nanobeam on the Visco-Pasternak bed based on the NT. They showed that an increase in the inhomogeneity coefficient and the wavenumbers reduced the phase velocity. Ma *et al*. (2017) studied the wave propagation in magneto-electro-elastic nanobeams using NT and both the TBM and EBM. They demonstrated that thermo-electro-magnetic loading causes a cut-off in the wavenumbers corresponding to the zero-wave frequency. Employing the NSGT, She *et al*. (2018) developed a model for analyzing wave propagation in porous nanobeams. They indicated that temperature variations and heterogeneity have significant effects on phase velocity. They also showed that the phase velocity could be reduced or increased depending on the porosity volume fraction and the power-law index values. Al-Furjan *et al*. (2021) analyzed the wave propagation of nano-composite doubly curved panel embedded in the viscoelastic foundation based on Higher-order shear deformable theory (HSDT). They reported that the effects of fiber angle and damping parameters on the phase velocity are dependent on the wavenumber. Shahsavari *et al*. (2023) investigated the effects of viscosity on wave propagation in a viscoelastic system of curved P-FGM nanobeams based on NSGT. They showed that although the effect of the viscosity coefficient is more complicated at larger wavenumbers, in general, increasing the viscosity coefficient leads to earlier damping of the system. Also, Boyina and Piska (2023) modeled viscoelastic Timoshenko nanobeams based on NSGT and investigated the effects of surface stress and magnetic field on its phase velocity and damping ratio.

In the present study, thermal effects on wave propagation in the curved nanobeam are investigated. Mechanical properties of the curved nanobeam are assumed to be functions of temperature. The curved nanobeam is modeled using the first-order shear deformation theory (FSDT), and its dynamic behavior is investigated employing the NSGT. Furthermore, the results are compared with CT, SGT, and NT. For this purpose, using Hamilton's principle, the governing equations are derived and analytically solved. Using the proposed model, we study the effects of the geometry, material properties, thermo-mechanical, strain gradient, and nonlocal parameters on the phase velocity of the curved nanobeam, and the results are discussed in detail.

2. Materials and methods

This section presents concepts related to material description, curved nanobeam modeling, and the study of its thermo-dynamic behavior. As can be seen in Fig. 1, the length of the curved nanobeam, width, and height (thickness) of its cross-section are introduced by L, b, and h, respectively. R is the radius of the curved nanobeam. The relation between the length and radius of the curved nanobeam is as $L=R\beta$. According to this relation, for a constant length, an increase in the radius causes to decrease in the angle, and finally, the curved nanobeam becomes a straight nanobeam. γ represents the curvature angle and $s=R\gamma$. According to Fig. 1, Cartesian coordinates are used to define positions on the curved nanobeam. The s-axis is along the neutral axis of the curved nanobeam. The y-axis is outward, perpendicular to the plane. The z-axis is towards the center of curvature (O), perpendicular to the s-y plane.

2.1 Nonlocal strain gradient elasticity theory

The classical theories are inefficient for studying the mechanical behavior of small-scale nanostructures. Consequently, the NSGT is used to capture the small-size

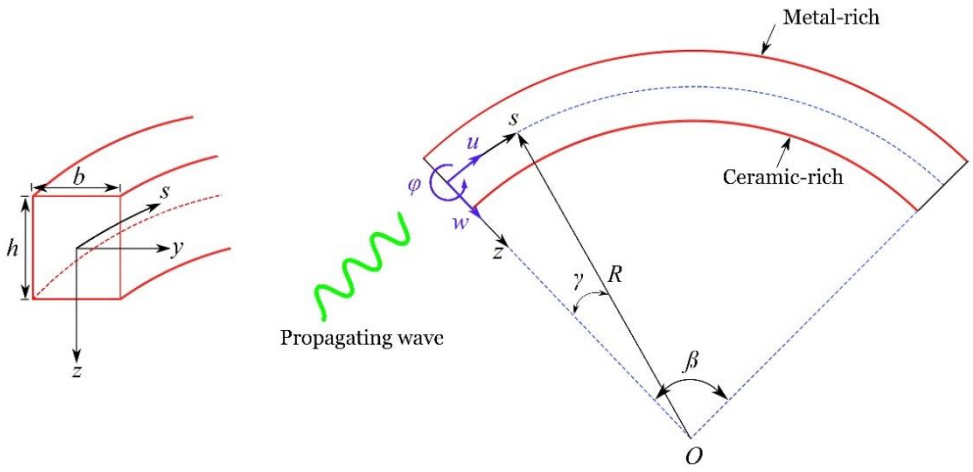

Fig. 1 The geometry of the curved nanobeam on the Cartesian coordinates

Table 1 Stress-strain equations based on values of l and μ corresponding to elasticity theories.

Theory	CT	SGT	NT	NSGT
Strain gradient parameter (l)	= 0	≠ 0	= 0	≠ 0
Nonlocal parameter (μ)	= 0	= 0	≠ 0	≠ 0
Stress-strain relation	$t_{ss} = E\varepsilon_{ss}$	$t_{ss} = E\aleph\varepsilon_{ss}$	$\Im t_{ss} = E\varepsilon_{ss}$	$\Im t_{ss} = E\aleph\varepsilon_{ss}$

effects. According to this theory (Lim *et al.* 2015, Lu *et al.* 2017), total stress is defined as

$$t_{ss} = \sigma_{ss} - \partial_s \sigma_{ss}^{(1)} \tag{1}$$

where σ_{ss} represents the classical stress and superscript $(\cdot)^{(1)}$ represents the nonlocal stress component defined as follows

$$\sigma_{ss} = \int_0^L E\eta_0(s,s',e_0a)\varepsilon'_{ss}(s')ds' \tag{2}$$

$$\sigma_{ss}^{(1)} = l^2 \int_0^L E\eta_1(s,s',e_1a)\partial_s\varepsilon'_{ss}(s')ds' \tag{3}$$

Here, E is Young's modulus. ε'_{ss} and $\partial_s\varepsilon'_{ss}$ are the local strain and its gradient, respectively. $\eta_0(s,s',e_0a)$ and $\eta_1(s,s',e_1a)$ are the nonlocal kernel functions. E_0a and e_1a are the nonlocal parameters. Also, l is the length scale parameter revealing the strain gradient effects. According to (Li *et al.* 2015, Lim *et al.* 2015), the general differential form of bi-Helmholtz nonlocal strain gradient elasticity theory is expressed as

$$\begin{aligned}&[1-(e_1a)^2\partial_s^2][1-(e_0a)^2\partial_s^2]t_{ss} = \\ &[1-(e_1a)^2\partial_s^2]\varepsilon_{ss} - El^2[1-(e_0a)^2\partial_s^2]\partial_s^2\varepsilon_{ss}\end{aligned} \tag{4}$$

It can be shown in the form

$$\Im_1\Im_0 t_{ss} = E\Im_1\varepsilon_{ss} - El^2\Im_0\partial_s^2\varepsilon_{ss} \tag{5}$$

in which $\Im_i$ denotes the nonlocal operator and is defined as

$$\Im_i = 1-(e_ia)^2\nabla^2, \quad i = 0,1 \tag{6}$$

where $\nabla^2(=\partial^2_s)$ stands for Laplace operator. Finally, considering $e_0a=e_1a=\mu$ for simplicity, Eq. (5) is obtained as

$$\Im t_{ss} = E\aleph\varepsilon_{ss}, \quad \Im_1 = \Im_0 = \Im \tag{7}$$

where $\aleph$ is the strain gradient operator, which is defined as

$$\aleph = 1 - l^2\nabla^2 \tag{8}$$

Regarding the values of l and μ parameters, Table 1 presents the stress-strain equations based on CT, SGT, NT, and NSGT theories.

2.2 Thermal distribution expansion

The curved nanobeam made of a functionally graded combination of metal and ceramic is shown in Fig. 1.

In order to study the thermo-dynamic behavior of the curved nanobeam in an environment with thermal gradients, the thermal dependency of materials should be taken into account. Thermo-elastic properties of materials can be defined as a function of temperature as follows (Shen 2016, Alazwari *et al.* 2022):

$$\Re_f(T) = \Re_0(\Re_{-1}T^{-1} + 1 + \Re_1T + \Re_2T^2 + \Re_3T^3) \tag{9}$$

The subscript f could be *c* and *m*, representing the properties of ceramic and metal phases, respectively. $\Re_i$ (i=-1, 0, 1, 2, 3) are the thermal constants. Constitutive properties of FGMs are defined as follows

$$\begin{aligned}\Re(z,T) &= \Re_m(T) + \Re_{mc}(T)V_c(z), \\ \Re_{mc} &= \Re_c - \Re_m\end{aligned} \tag{10}$$

where V_c and V_m are volume fractions of ceramic and metal phases, respectively, introduced as (Alazwari *et al.* 2022)

$$\begin{aligned}V_c &= \left(0.5 + \frac{z}{h}\right)^k, \\ V_m &= 1 - \left(0.5 + \frac{z}{h}\right)^k, \\ V_c + V_m &= 1\end{aligned} \tag{11}$$

Table 2 Temperature-dependent mechanical properties of the FG materials (Reddy and Chin 1998, Alazwari *et al.* 2022)

Material	Properties	$\Re_{-1}$	$\Re_0$	$\Re_1$	$\Re_2$	$\Re_3$
SUS304 (metal phase)	*E (Pa)*	0	201.040×10^{9}	3.079×10^{-4}	-6.534×10^{-7}	0
	v	0	0.326	-2.002×10^{-4}	3.797×10^{-7}	0
	ρ (kgm^{-3})	0	8166.000	0	0	0
	α (K^{-1})	0	12.330×10^{-6}	8.086×10^{-4}	0	0
	K (Wm^{-1}K^{-1})	0	15.379	-1.264×10^{-3}	2.092×10^{-6}	-7.223×10^{-10}
Si_3N_4 (ceramic phase)	*E (Pa)*	0	348.430×10^{9}	-3.070×10^{-4}	2.160×10^{-7}	-8.946×10^{-11}
	v	0	0.240	0	0	0
	ρ (kgm^{-3})	0	2170.000	0	0	0
	α (K^{-1})	0	5.8723×10^{-6}	9.095×10^{-4}	0	0
	K (Wm^{-1}K^{-1})	0	13.723	-1.032×10^{-3}	5.466×10^{-7}	-7.876×10^{-11}

where *k* stands for the power-law index. According to Eq. (10), the properties, including Young's modulus (E), Poisson's ratio (v), density (ρ), thermal expansion coefficient (α), and bulk modulus (G), are defined as functions of T and z ($\Re=E, v, \rho, \alpha; G=f(E, v)$). The thermal constants related to the thermo-elastic characteristics are presented in Table 2. In general, the one-dimensional steady-state heat conduction equation in the direction of the curved nanobeam thickness is (Kiani *et al.* 2011, Ebrahimi *et al.* 2019b)

$$\partial_z(K(z)\,\partial_z T) = 0 \tag{12}$$

where T stands for the temperature, and $K(z)$ is the thermal conductivity which is defined as follows (Komeili *et al.* 2011)

$$K(z) = K_m + K_{mc}\left(0.5 + \frac{z}{h}\right)^k, \quad K_{mc} = K_c - K_m \tag{13}$$

Here, K_c and K_m stand for ceramic and metal thermal conductivities, respectively. In this study, the effect of two types of thermal loadings is investigated. The temperature function of the thermal loadings is obtained by solving Eq. (12).

2.2.1 Heat Conduction (HC):

In the case of one-dimensional heat conduction, surfaces of the curved nanobeam experience constant temperatures introducing a temperature gradient along the curved nanobeam thickness.

$$T\left(\frac{h}{2}\right) = T_c, \quad T\left(-\frac{h}{2}\right) = T_m \tag{14}$$

Here, T_c and T_m are the uniformly distributed temperatures at ceramic-rich and metal-rich surfaces, respectively. As represented (Komijani *et al.* 2014), the temperature function of HC thermal loading is obtained based on the thermal boundary conditions introduced in Eq. (14).

$$T_{HC} = T_m + T_{mc}\left(\frac{\Xi}{\Theta}\right), \; T_{mc} = T_c - T_m \tag{15}$$

where Ξ and Θ are obtained, respectively, as follows (Komijani *et al.* 2014)

$$\Xi = \sum_{i=0}^{n}\left[\frac{1}{ik+1}\left(-\frac{K_{mc}}{K_m}\right)^i\left(\frac{1}{2}+\frac{z}{h}\right)^{ik+1}\right] \tag{16}$$

$$\Theta = \sum_{i=0}^{n}\left[\frac{1}{ik+1}\left(-\frac{K_{mc}}{K_m}\right)^i\right] \tag{17}$$

2.2.2 Uniform Temperature Rise (UTR):

In this case, it is considered that the ceramic-rich and metal-rich surfaces experience a constant temperature, and the curved nanobeam is exposed to the non-dimensional temperature ($T_c=T_m=T_{UTR}$). As a result, Eq. (16) is simplified, and the temperature function of UTR thermal loading becomes $T_{HC}=T_{UTR}$. It is noted that there is a temperature difference between the environment and the curved nanobeam as (Kiani *et al.* 2011)

$$\Delta T = T_\theta - T_0 \tag{18}$$

Here, θ could be HC or UTR, and T_0 is the constant ambient temperature.

2.3 Governing equations

Based on the FSDT, the displacements of an arbitrary point of curved nanobeam along the coordinate axes are (Zhao and Yu 2021)

$$u_s = u(s,t) - z\varphi(s,t), \;\; u_y = 0, \;\; u_z = w(s,t) \tag{19}$$

where t stands for time. As shown in Fig. 1, u and w are the displacement components, and φ is the rotation of the midplane. According to the concepts in Continuum Mechanics (Lai *et al.* 2009, Liu and Reddy 2011), for curved nanobeams, strain components are defined as

$$\varepsilon_{ss} = \partial_s u_s + \frac{u_z}{R} \tag{20}$$

$$\gamma_{sz} = \partial_z u_s + \partial_s u_z - \frac{u_s}{R} \tag{21}$$

Based on the assumption that the radius of the curved nanobeam is much larger than its thickness (i.e., $|z/R|<<1$),

strain components are obtained as

$$\varepsilon_{ss} = \partial_s u - z\partial_s \varphi + \frac{w}{R} \tag{22}$$

$$\gamma_{sz} = \partial_s w - \varphi - \frac{u}{R} \tag{23}$$

All other strain components are zero. The governing equations will be derived using Hamilton's principle (Bensaid *et al*. 2018, Ganapathi and Polit 2018, Matouk *et al*. 2020)

$$\delta H = \int_{t_0}^{t_1} (\delta U_S - \delta U_T + \delta U_W) dt = 0 \tag{24}$$

According to the NSGT, a variational form of strain energy density is presented as follows (She *et al.* 2018)

$$\delta U_S = \int_V \begin{Bmatrix} \sigma_{ss}\delta\varepsilon_{ss} + \sigma_{ss}^{(1)}\partial_s\delta\varepsilon_{ss} + \\ k_s\tau_{sz}\delta\gamma_{sz} + k_s\tau_{sz}^{(1)}\partial_s\delta\gamma_{sz} \end{Bmatrix} dV \tag{25}$$

where k_s is the shear correction factor, equal to 5/6 (Komijani *et al.* 2014). Substituting Eqs. (1), (22)-(23) into Eq. (25) and performing mathematical manipulations, we obtain the strain energy density in the form of

$$\begin{aligned} \delta U_S = & \int_0^L \begin{Bmatrix} N\delta\left(\partial_s u + \frac{w}{R}\right) - M\delta(\partial_s\varphi) \\ +Q\delta\left(\partial_s w - \varphi - \frac{u}{R}\right) \end{Bmatrix} ds \\ & + \begin{bmatrix} N^{(1)}\delta\left(\partial_s u + \frac{w}{R}\right) - M^{(1)}\delta(\partial_s\varphi) \\ +Q^{(1)}\delta\left(\partial_s w - \varphi - \frac{u}{R}\right) \end{bmatrix}_0^L \end{aligned} \tag{26}$$

where *N*, *M*, and *Q* are stress resultants related to normal force, moment, and shear force, respectively (Rahmani *et al.* 2017, She *et al.* 2018, Xing *et al.* 2022). Superscript (□) $^{(1)}$ represents the nonlocal stress resultants.

$$\{N, M, Q\} = \int_A \{t_{ss}, zt_{ss}, k_s t_{sz}\} dA \tag{27}$$

$$\left\{N^{(1)}, M^{(1)}, Q^{(1)}\right\} = \int_A \left\{\sigma_{ss}^{(1)}, z\sigma_{ss}^{(1)}, k_s\tau_{sz}^{(1)}\right\} dA \tag{28}$$

The variational form of kinetic energy is presented in the form

$$\delta U_T = \int_V \rho \begin{Bmatrix} \partial_t u\delta(\partial_t u) + z^2\partial_t\varphi\delta(\partial_t\varphi) \\ -z[\partial_t u\delta(\partial_t\varphi) + \partial_t\varphi\delta(\partial_t u)] \\ +\partial_t w\delta(\partial_t w) \end{Bmatrix} dV \tag{29}$$

$$\delta U_T = \int_0^L \begin{Bmatrix} I_0[\partial_t u\delta(\partial_t u) + \partial_t w\delta(\partial_t w)] \\ -I_1[\partial_t u\delta(\partial_t\varphi) + \partial_t\varphi\delta(\partial_t u)] \\ +I_2\partial_t\varphi\delta(\partial_t\varphi) \end{Bmatrix} ds \tag{30}$$

I_0, I_1, and I_2 are the inertia moments defined as follows

$$\{I_0, I_1, I_2\} = \int_A \rho(z,T)\{1, z, z^2\} dA \tag{31}$$

The variational form of external work applied to the curved nanobeam is

$$\delta U_W = \int_0^L \{q\delta w + N^T\partial_s w\delta(\partial_s w)\} ds \tag{32}$$

where *q* represents the transverse loading imposed on the curved nanobeam. In this study, it is assumed that the thermal loading affects the thermo-dynamic behavior of the curved nanobeam as external work. The thermal resultant for both types of thermal loadings mentioned in Section 2.2 is (Matouk *et al.* 2020, Alazwari *et al.* 2022)

$$N^T = \int_A E(z,T)\alpha(z,T)\Delta T dA \tag{33}$$

Substituting Eqs. (26), (30), and (32) into Eq. (24) and performing mathematical manipulations, we derive the governing equations as follows

$$\delta u: \quad \partial_s N + \frac{Q}{R} - I_0\partial_t^2 u + I_1\partial_t^2\varphi = 0 \tag{34}$$

$$\delta w: \quad -\frac{N}{R} + \partial_s Q - q + N^T\partial_s^2 w - I_0\partial_t^2 w = 0 \tag{35}$$

$$\delta\varphi: \quad -\partial_s M + Q + I_1\partial_t^2 u - I_2\partial_t^2\varphi = 0 \tag{36}$$

Also, simply supported boundary conditions (at γ=0, β) for the curved nanobeam are given by

$$\begin{aligned} & u = 0 \text{ or } N = 0, \\ & w = 0 \text{ or } Q = 0, \\ & \varphi = 0 \text{ or } M = 0 \end{aligned} \tag{37}$$

Based on NSGT, considering Eqs. (8), (22)-(23) the stress-strain relations become

$$\begin{aligned} \Im t_{ss} = & E(z,T)\aleph\varepsilon_{ss} = \\ & E(z,T)\aleph\left(\partial_s u - z\partial_s\varphi + \frac{w}{R}\right) \end{aligned} \tag{38}$$

$$\begin{aligned} \Im t_{sz} = & G(z,T)\aleph\gamma_{sz} = \\ & G(z,T)\aleph\left(\partial_s w - \varphi - \frac{u}{R}\right) \end{aligned} \tag{39}$$

The stress resultants are obtained by performing mathematical manipulations on Eqs. (38)-(39) as follows

$$\begin{aligned} N = & \mu^2\partial_s^2 N + \aleph\left(A\left(\partial_s u + \frac{w}{R}\right) - B\partial_s\varphi\right) = \\ & (1-\Im)N + \aleph\left(A\left(\partial_s u + \frac{w}{R}\right) - B\partial_s\varphi\right) \end{aligned} \tag{40}$$

$$\begin{aligned} M = & \mu^2\partial_s^2 M + \aleph\left(B\left(\partial_s u + \frac{w}{R}\right) - D\partial_s\varphi\right) = \\ & (1-\Im)M + \aleph\left(B\left(\partial_s u + \frac{w}{R}\right) - D\partial_s\varphi\right) \end{aligned} \tag{41}$$

$$\begin{aligned} Q = & \mu^2\partial_s^2 Q + \aleph C\left(\partial_s w - \varphi - \frac{u}{R}\right) = \\ & (1-\Im)Q + \aleph C\left(\partial_s w - \varphi - \frac{u}{R}\right) \end{aligned} \tag{42}$$

where *A*, *B*, *C*, and *D* are the stiffness coefficients defined as follows

$$\begin{aligned} \{A, B, D\} = & \int_A E(z,T)\{1, z, z^2\} dA\,, \\ C = & \int_A G(z,T) dA \end{aligned} \tag{43}$$

Substituting Eqs. (40)-(42) into Eqs. (34)-(36), we obtain the final form of the governing equations

Table 3 The form and value of the small-scale parameter (Z; Eq. (54)) based on elasticity theories

Theory	Form of Z	Value of Z
CT	1	1
SGT	$1-l^2\partial_s^2$	$1+\mu^2\zeta^2$
NT	$1/(1-\mu^2\partial_s^2)$	$1/(1+\mu^2\zeta^2)$
NSGT	$(1-l^2\partial_s^2)/(1-\mu^2\partial_s^2)$	$(1+l^2\zeta^2)/(1+\mu^2\zeta^2)$

$$\delta u:\ \aleph\begin{bmatrix}A\left(\partial_s^2 u+\frac{\partial_s w}{R}\right)-B\partial_s^2\varphi\\ +\frac{C}{R}\left(\partial_s w-\varphi-\frac{u}{R}\right)\end{bmatrix}+\Im(-I_0\partial_t^2 u+I_1\partial_t^2\varphi)=0 \tag{44}$$

$$\delta w:\ \aleph\begin{bmatrix}-\frac{A}{R}\left(\partial_s u+\frac{w}{R}\right)+\frac{B}{R}\partial_s\varphi\\ +C\left(\partial_s^2 w-\partial_s\varphi-\frac{\partial_s u}{R}\right)\end{bmatrix}+\Im(N^T\partial_s^2 w-q-I_0\partial_t^2 w)=0 \tag{45}$$

$$\delta\varphi:\ \aleph\begin{bmatrix}-B\left(\partial_s^2 u+\frac{\partial_s w}{R}\right)+D\partial_s^2\varphi\\ +C\left(\partial_s w-\varphi-\frac{u}{R}\right)\end{bmatrix}+\Im(I_1\partial_t^2 u-I_2\partial_t^2\varphi)=0 \tag{46}$$

In the following, the wave propagation in the curved nanobeam and its thermo-dynamic behavior is studied. For this purpose, results will be presented and compared based on the theories mentioned in Table 1.

3. Solution procedure

To solve governing equations (Eqs. (44)-(46)), the displacement components (u, w) and rotation (φ) are defined as follows (Faroughi *et al.* 2020, Shahsavari *et al.* 2023)

$$u=\underline{U}\,exp[i(\zeta s-\omega t)] \tag{47}$$

$$w=\underline{W}\,exp[i(\zeta s-\omega t)] \tag{48}$$

$$\varphi=\underline{\Phi}\,exp[i(\zeta s-\omega t)] \tag{49}$$

Here, $\underline{U}$, $\underline{W}$, and $\underline{\Phi}$ represent the wave amplitudes. ζ and ω stand for wavenumber and wave frequency, respectively. In the case of $q=0$, substituting Eqs. (47)-(49) in Eqs. (44)-(46), we obtain the governing equations in the form of

$$\delta u:\ \left[-A\zeta^2-\frac{C}{R^2}+\frac{\omega^2}{Z}I_0\right]\underline{U}+\left[\frac{A+C}{R}i\zeta\right]\underline{W}+\left[B\zeta^2-\frac{C}{R}-\frac{\omega^2}{Z}I_1\right]\underline{\Phi}=0 \tag{50}$$

$$\delta w:\ \left[-\frac{A+C}{R}i\zeta\right]\underline{U}+\left[\frac{B}{R}-C\right]i\zeta\underline{\Phi}-\left[\frac{A}{R^2}+C\zeta^2+\frac{N^T\zeta^2-\omega^2 I_0}{Z}\right]\underline{W}=0 \tag{51}$$

$$\delta\varphi:\ \left[B\zeta^2-\frac{C}{R}-\frac{\omega^2}{Z}I_1\right]\underline{U}-\left[\frac{B}{R}-C\right]i\zeta\underline{W}-\left[D\zeta^2+C-\frac{\omega^2}{Z}I_2\right]\underline{\Phi}=0 \tag{52}$$

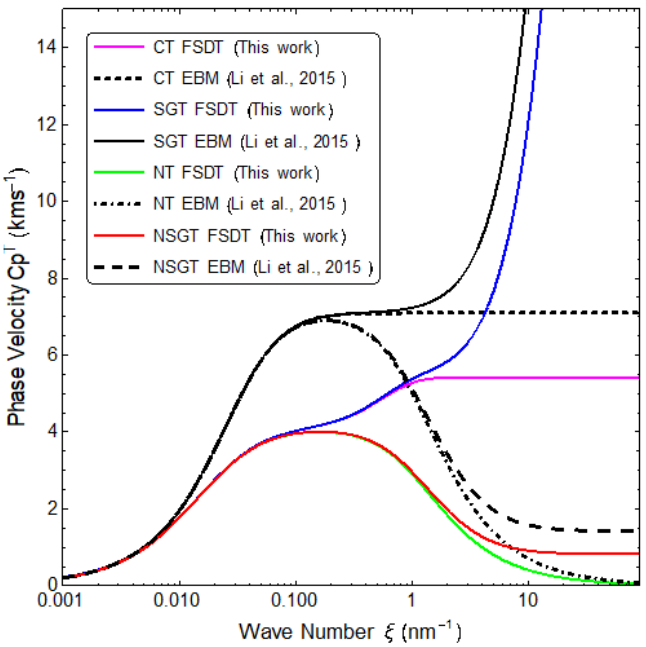

Fig. 2 The results of the FSDT compared to the results of the EBM (Li *et al.* 2015) for the geometrical parameters of b=1000 (nm), h=100 (nm), L/h=10, and k=1. The small-scale parameters are l=0, μ=0 for CT, l=0.2 (nm), μ=0 for SGT, l=0, μ=1 (nm) for NT, and l=0.2 (nm), μ=1 (nm) for NSGT

Afterward, the form of stiffness and mass matrices is formulated as follows

$$\left[\{\Gamma\}-\left(\frac{\omega^2}{Z}\right)\{\Upsilon\}\right]\{\underline{U}\quad\underline{W}\quad\underline{\Phi}\}^T=0 \tag{53}$$

Γ represents the stiffness matrix obtained from spatial derivatives related to the strain energy density and external work. Similarly, Υ is the mass matrix induced by time derivatives related to the kinetic energy. According to Eqs. (4)-(6), the ratio of the strain gradient operator to the nonlocal operator is defined as follows

$$Z=\frac{\aleph}{\Im}=\frac{(1-l^2\partial_s^2)}{(1-\mu^2\partial_s^2)} \tag{54}$$

Subsequently, considering the different values of l and μ in different theories aforementioned in Table 1, various forms and values for Z are given in Table 3.

Substitution of Eqs. (50)-(52) into Eq. (53) gives the coefficient matrix as

$$\begin{bmatrix}A\zeta^2+\frac{C}{R^2} & -\frac{A+C}{R}i\zeta & \frac{C}{R}-B\zeta^2\\ -\frac{A+C}{R}i\zeta & -\frac{A}{R^2}-C\zeta^2-\frac{N^T\zeta^2}{Z} & \left(\frac{B}{R}-C\right)i\zeta\\ \frac{C}{R}-B\zeta^2 & \left(\frac{B}{R}-C\right)i\zeta & C+D\zeta^2\end{bmatrix}-\frac{\omega^2}{Z}\begin{bmatrix}I_0 & 0 & -I_1\\ 0 & -I_0 & 0\\ -I_1 & 0 & I_2\end{bmatrix}=0 \tag{55}$$

Table 4 Comparison of the nanobeam wave frequency with the results of Ref. (Lu *et al.* 2017). b=1 (*nm*), h=1 (*nm*), L/h=10, k=0, k_s=5/6

n	l/h	μ=0 (*nm*)		μ=1 (*nm*)		μ=2 (*nm*)	
		This work	Ref. (Lu *et al.* 2017)	This work	Ref. (Lu *et al.* 2017)	This work	Ref. (Lu *et al.* 2017)
1	0	9.70748	9.7075	9.26121	9.2612	8.21964	8.2196
	0.5	9.82651	9.8265	9.37477	9.3748	8.32043	8.3204
	1	10.17530	10.1753	9.70748	9.7075	8.61572	8.6157
2	0	37.09620	37.0962	31.41050	31.4105	23.09890	23.0989
	0.5	38.88370	38.8837	32.92410	32.9241	24.21200	24.212
	1	43.81090	43.8109	37.09620	37.0962	27.28010	27.2801
3	0	78.15470	78.1547	56.87530	56.8753	36.62720	36.6272
	0.5	86.39780	86.3978	62.87400	62.874	40.49030	40.4903
	1	107.39600	107.3957	78.15470	78.1547	50.33100	50.331

In order to analyze the dynamic behavior of the curved nanobeam, the eigenvalue problem must be solved. In this regard, the wave frequency is obtained in terms of wave-number by solving Eq. (55) ($\omega=f_i(\zeta)$). Also, the phase velocity could be found by $C_p^i=f_i(\zeta)/\zeta$, (i=*T, L, S*) (Xing *et al.* 2022).

4. Results and discussion

This study investigates the effects of thermal loadings on wave propagation in the curved nanobeam. The desired beam model was developed based on FSDT and NSGT. Using Hamilton's principle, the governing equations and boundary conditions were derived. Finally, the effects of small-scale, geometrical, and thermo-mechanical parameters on the dynamic behavior of the curved nanobeam were analyzed and discussed in this section.

4.1 Validation

For the case where the nanobeam is assumed to be straight, the accuracy of the proposed model is verified in this section. For this purpose, a comparison study is conducted. Table 4 represents a comparative study of the wave frequency with the results of (Lu *et al.* 2017). The nanobeam is made of Aluminum with properties E=70 *(GPa)*, v=0.3, ρ=2702 (kg/m^3), and other parameters L=10 (nm), h=1 (nm), b=1 (nm), k=0. Regarding Table 4, an increase of μ and a decrease of l/h ratio led to a decrease in the wave frequency. It can be seen that there is a good agreement between the present results and those reported by (Lu *et al.* 2017).

For more verification, the wave propagation in a straight nanobeam is compared with the results of (Li *et al.* 2015), as shown in Fig. 2. Material properties are considered to be Steel E_m=210 (*GPa*), v_m=0.3, ρ_m=7800 (*kg/m*^{3}) and Al_2O_3 E_c=390 (*GPa*), v_c=0.24, ρ_c=3960 (*kg/m*^{3}), and other effective parameters h=100 (*nm*), L/h=10, b=1000 (*nm*), k=1. It is noted that (Li *et al.* 2015) used the Euler-Bernoulli beam model (EBM). In this work, the nanobeam is modeled based on FSDT. It can be observed that the phase velocity follows a similar pattern. However, the results for the FSDT are less than those estimated by (Li *et al.* 2015). This phenomenon occurs due to neglecting the effects of shear deformations in the EBM. Similar results can be seen in (She *et al.* 2018). Based on Fig. 2, it is revealed that the proposed model is validated. Also, the difference between the results of EBM and FSDT is evident.

4.2 Parametric study

Using the proposed model, we analyze the wave propagation in the curved nanobeam as shown in Fig. 1. A longitudinal wave is propagated in the simply supported curved nanobeam with *thickness* h=100 (nm) and width b=60 (nm), which is exposed to different thermal loadings. In this case, the thermo-mechanical properties of the FG curved nanobeam are presented in Table 2.

4.2.1 Small-scale parameters effect

Fig. 3 reveals the effects of the small-scale parameters, including strain gradient and nonlocal, on the phase velocity of the curved nanobeam based on CT, SGT, NT, and NSGT. In this regard, L/h=10, k=1, ΔT=0 (*K*), and $\gamma=\pi/3$. As can be seen in Figs. 3(a)-(f), when Z<1, the stiffness-softening occurs in the curved nanobeam. Subsequently, the NSGT predicts the phase velocity is less than the values calculated based on the CT. While for Z>1, the effect of the stiffness-hardening appears; thus, different results are observed. Instead, when Z=1, both theories predict similar results. In this condition, the strain gradient and nonlocal parameters neutralize each other.

From Fig. 3, it is clear that the phase velocity value strongly depends on the wavenumber. Based on the utilized theories, the difference in the phase velocity values manifests in large wavenumbers. Conversely, all theories predict the same results in small wavenumbers. It is noted that these theories have been upgraded to capture the behavior of the material on small scales with the help of small-scale parameters. Therefore, when a wave is propagated the curved nanobeam, these theories can predict its behavior at large wavenumbers (small wavelengths).

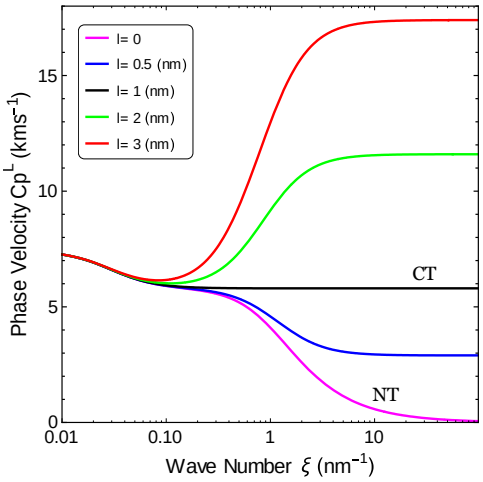

(a) The longitudinal wave C^L_p, μ=1 (*nm*)

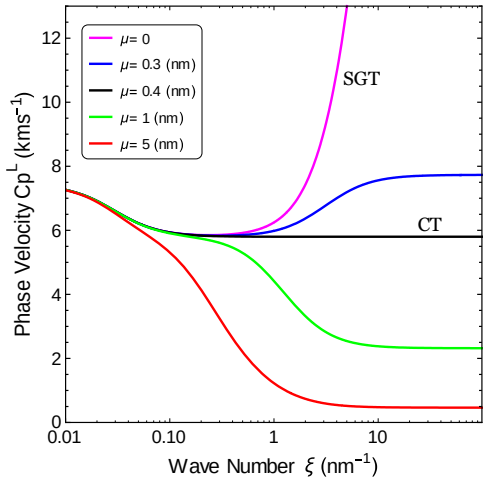

(b) The longitudinal wave C^L_p, l=0.4 (*nm*)

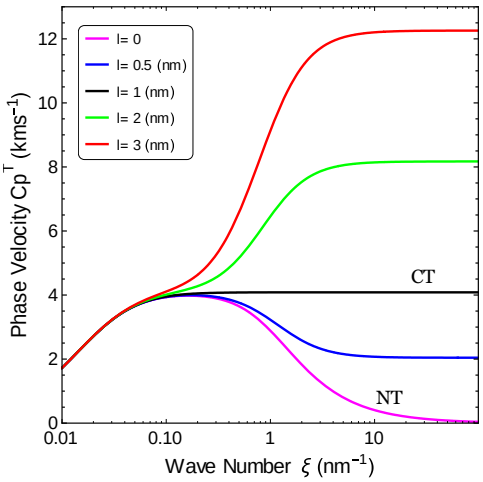

(c) The flexural wave C^T_p, μ=1 (*nm*)

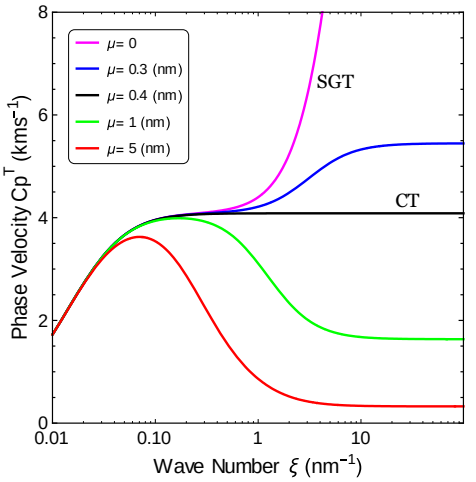

(d) The flexural wave C^T_p, l=0.4 (*nm*)

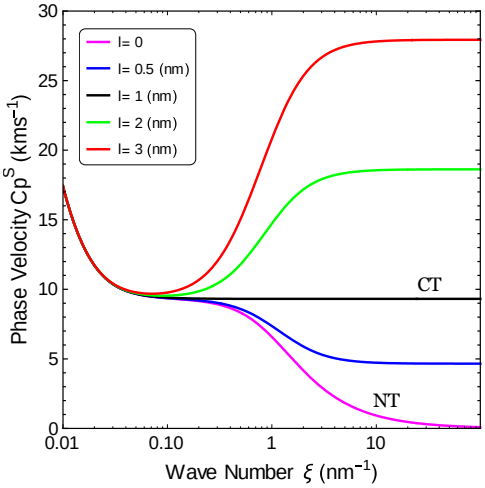

(e) The shear wave C^S_p, μ=1 (*nm*)

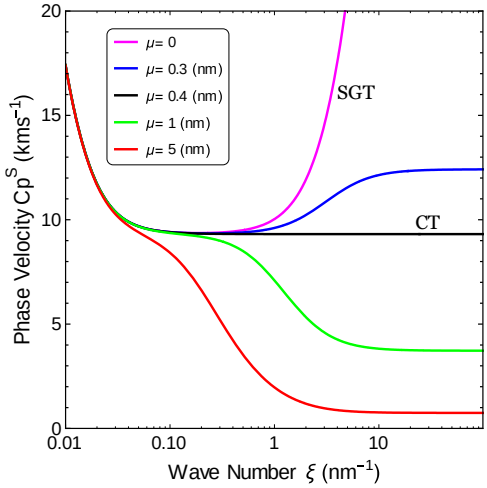

(f) The shear wave C^S_p, l=0.4 (*nm*)

Fig. 3 The phase velocity of (a) and(b) longitudinal, (c) and (d) flexural, (e) and (f) shear waves versus wavenumber corresponding to different values of l and μ representing CT, SGT, NT, and NSGT. The geometrical parameters are L/h=10, k=1, ΔT=0 (*K*) and $\gamma=\pi/3$

Approximately from wavenumber 10 onwards, CT and NSGT estimate a constant value for the phase velocity. However, as the wavenumber increases, the phase velocity based on the NT gradually decreases to zero. Although, based on the SGT, the phase velocity tends to infinity. This is due to the stiffness-softening/hardening effects. With the higher l and μ values, the phase velocity becomes more sensitive to the wavenumber variations. Also, the NSGT

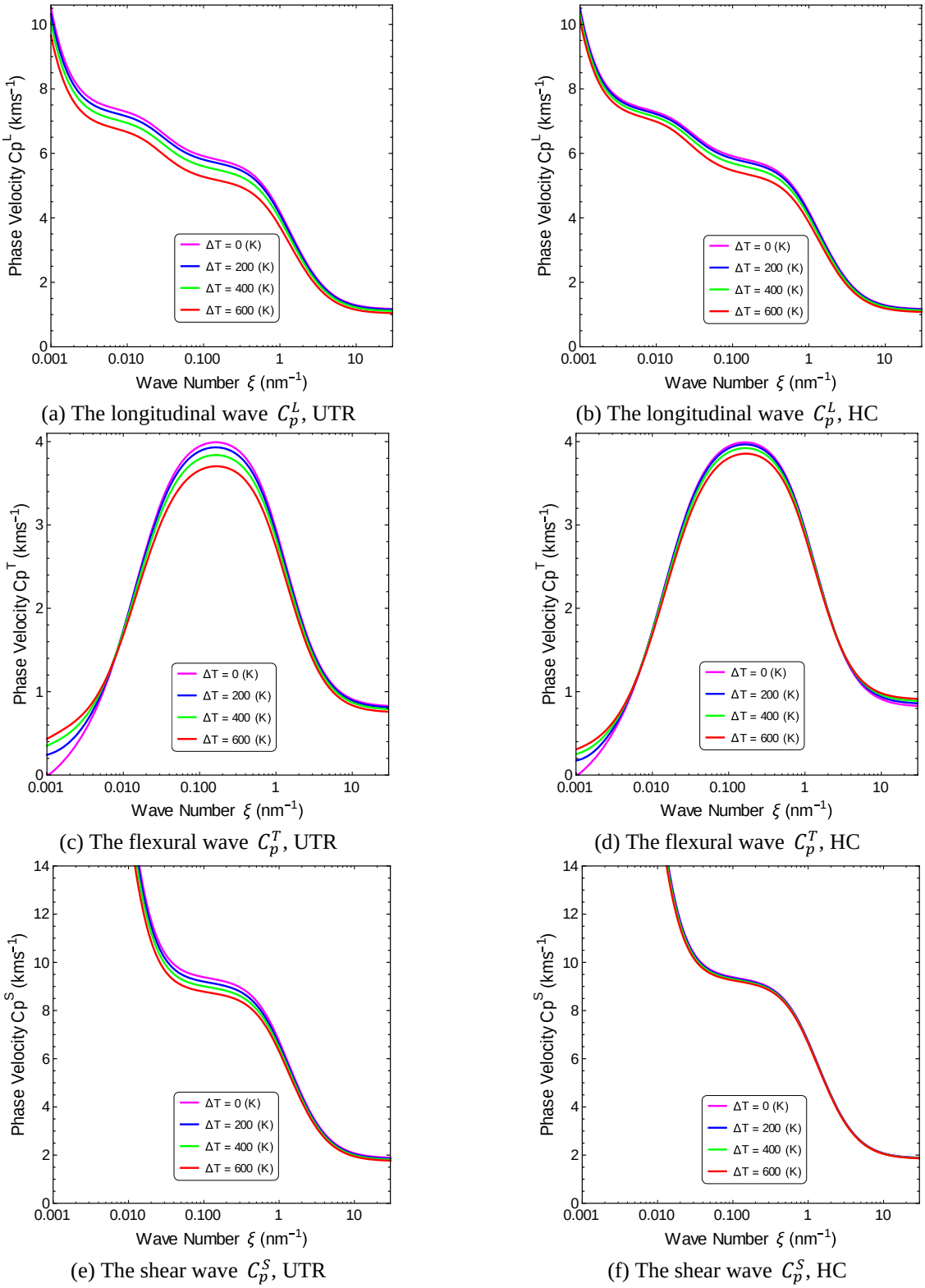

(a) The longitudinal wave C_p^L, UTR (b) The longitudinal wave C_p^L, HC

(c) The flexural wave C_p^T, UTR (d) The flexural wave C_p^T, HC

(e) The shear wave C_p^S, UTR (f) The shear wave C_p^S, HC

Fig. 4 The effects of UTR and HC thermal loadings on the phase velocity of (a) and (b) longitudinal, (c) and (d) flexural, (e) and (f) shear waves, based on the NSGT. The parameters of the nanobeam are L/h=10, l=0.2 (*nm*), μ=1 (*nm*), k=1, $\gamma=\pi/3$, T_0=273 (*K*), T_c=273 (*K*)

predicts phase velocity changes for smaller wavenumbers (larger wavelengths). A comparison of the results reveals that the strain gradient parameter (l) affects the phase velocity more than the nonlocal parameter (μ).

4.2.2 Thermal loadings effect

Based on the NSGT, Fig. 4 shows the effects of Uniform Temperature Rise (UTR) and Heat Conduction (HC) thermal loadings on the wave propagation in the curved

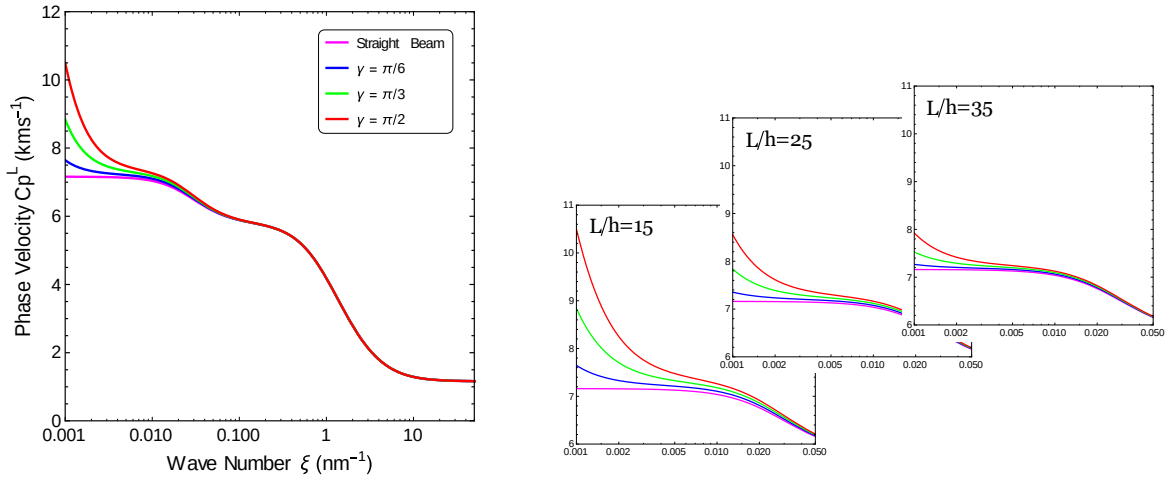

(a) The longitudinal wave C^L_p

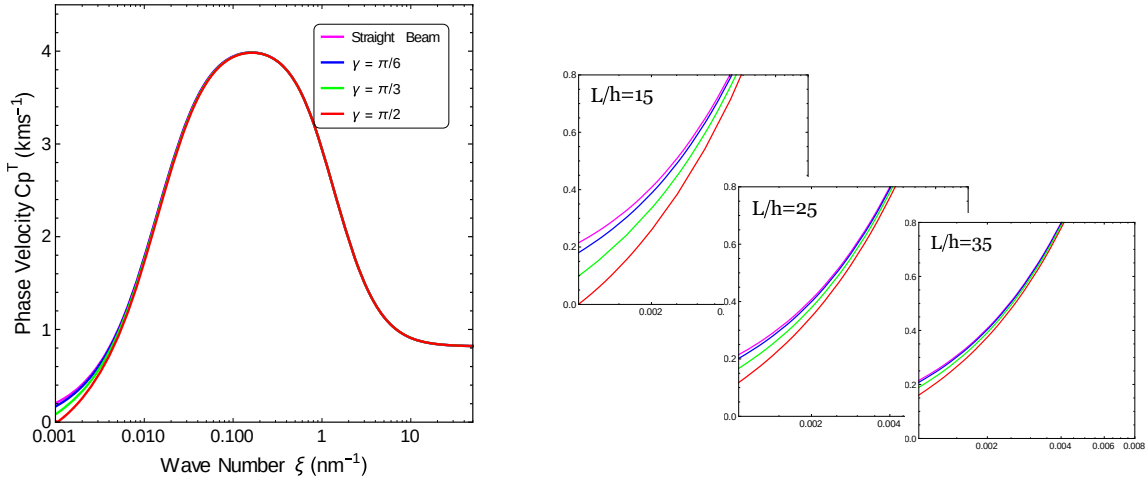

(b) The flexural wave C^T_p

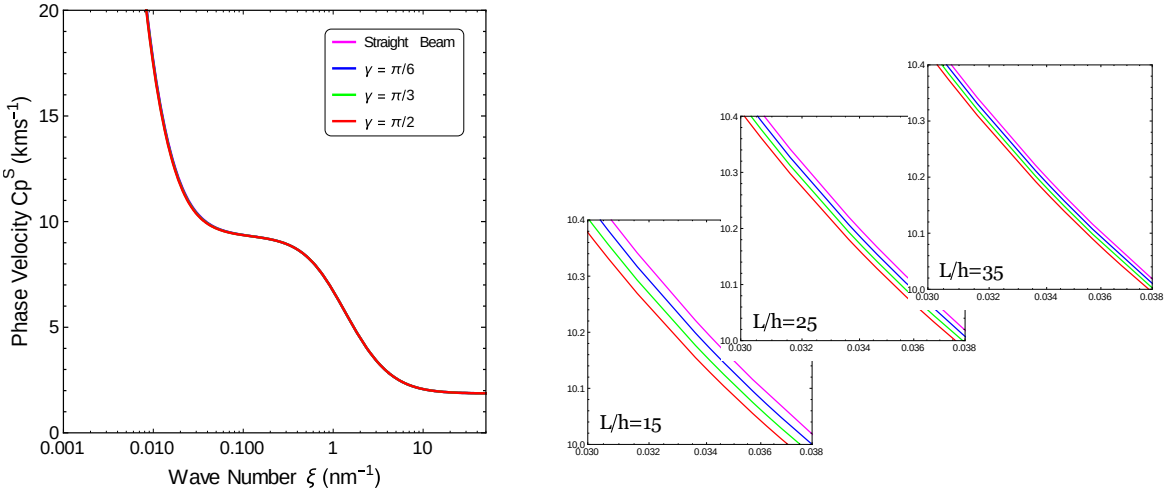

(c) The shear wave C^S_p

Fig. 5 Effects of the curved nanobeam arc angle and *L/h* ratio on the phase velocity for (a) longitudinal, (b) flexural, and (c) shear waves based on the NSGT. The parameters are l=0.2 (*nm*), μ=1 (*nm*), ΔT=0 (*K*), and k=1

nanobeam. In this case, L/h=10, $Z<1$, k=1, $\gamma=\pi/3$, T_0=273 (*K*), T_c=273 (*K*) is considered. It is observed that for both types of different thermal loadings, in a constant wave-number, with an increase in ΔT, the phase velocity decreases exponentially. In addition, increasing ΔT reduces the sensitivity of the phase velocity to the wavenumber changes. This behavior is evident for $\zeta \leq 1$. As can be observed, approximately within the $1 \leq \zeta \leq 10$ range, the value of phase velocity gradually decreases until it tends to a constant value, nearly from $10 \leq \zeta$ onwards. In general,

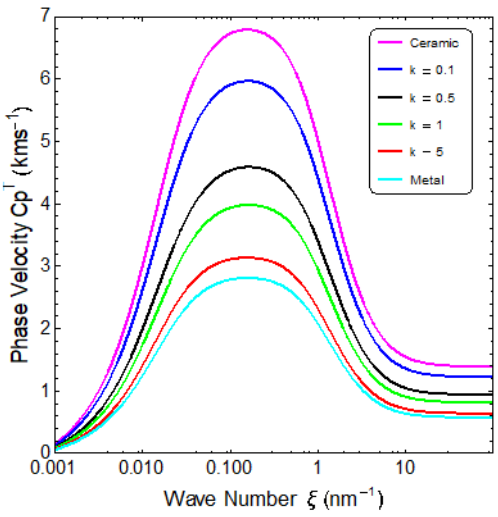

Fig. 6 Effect of the power-law index (k) on the phase velocity of the flexural wave (C^T_p), based on the NSGT. Thegeometrical parameters L/h=15, ΔT=0 (K), $\gamma=\pi/3$, and $Z<1$

thermal loadings have more effects on phase velocity in smaller wavenumbers.

An increase in the ambient temperature in the thermal loadings causes the effect of the stiffness-softening phenomenon. In this regard, compared to UTR thermal loading, HC thermal loading has less effect on the phase velocity. Also, as indicated in Figs. 4(a)-(d), it is revealed that the thermal loadings remarkably affect the phase velocity of longitudinal and flexural waves. But, as shown in Figs. 4 (e) and (f), the phase velocity of the shear wave is less dependent on the temperature changes (ΔT).

4.2.3 Arc angle effect

Based on the NSGT, the effect of the arc angle of the curved nanobeam (γ) on the phase velocity is shown in Figs. 5(a)-(c) for longitudinal, flexural, and shear waves, respectively. In this case, $Z<1$, ΔT=0 (K), and k=1 is considered. It is observed that for the small wavenumbers, the effect of the arc angle is evident. In this way, increasing the arc angle causes the phase velocity to experience more changes. For the longitudinal waves, the sensitivity of the phase velocity to the arc angle changes is remarkable (Fig. 5 (a)). Results indicate that increasing the arc angle causes an increase in the phase velocity of the longitudinal waves. Conversely, this phenomenon has a different effect on the phase velocity of flexural and shear waves (Figs. 5(b)-(c)). In this regard, the phase velocity of the shear waves shows fewer fluctuations (Fig. 5 (c)). In addition, it is observed that, for lower values of the L/h ratio, the phase velocity is more sensitive to the arc angle variations, which can be seen in all three cases.

4.2.4 Power-law index effect

Based on the NSGT, the effects of materials distribution (represented by the power-law index, k) on the flexural wave phase velocity are shown in Fig. 6. In this case, L/h=15, ΔT=0 (K), $\gamma=\pi/3$, and $Z<1$. It is observed that the higher the k value, the lower the sensitivity of the phase velocity to increase the wavenumber for $0.001\leq\zeta\leq10$. In other words, the higher the percentage of ceramic, the more governing the effect of the stiffness-hardening, and the more increase in phase velocity. Thus, when the FG curved nanobeam is entirely composed of ceramic or metal, the flexural wave propagates with the highest or lowest phase velocities, respectively.

5. Conclusions

This study investigates the wave propagation in the curved nanobeam which is exposed to different thermal loadings. For this purpose, a longitudinal wave perpendicular to the cross-sectional area of the simply supported curved nanobeam is propagated. The small-scale parameter, Z, collectively representing the strain gradient and the nonlocal parameters, is used in the proposed model based on the nonlocal strain gradient theory (NSGT). The governing equations of the proposed model are obtained using Hamilton's principle and solved analytically. As special cases of NSGT, the results based on classical, strain gradient, and nonlocal theories are presented and compared. Also, the effects of Uniform Temperature Rise (UTR) and Heat Conduction (HC) thermal loadings, the arc angle, geometric parameter (L/h), and the power-law index (k) on the wave propagation in the FG curved nanobeam and its thermo-dynamic behavior are investigated. The results are validated with those available in the previous works. Finally, the remarkable findings of this study are summarized as follows:

- The effect of small-scale parameters on the phase velocity is observed in large wavenumbers ($0.1\leq\zeta$). However, the effects of thermal loadings, arc angle, and L/h ratio are more visible in small wavenumbers (almost in $\zeta\leq1$ and $\zeta\leq0.01$, respectively). Instead, the effect of the power-law index is evident for all wavenumbers.
- When $Z<1$, the phase velocity decreases, and the stiffness-softening phenomenon occurs in the curved nanobeam. Conversely, when $Z>1$, the phase velocity increases, and the stiffness-hardening phenomenon occurs. In this regard, the strain gradient parameter (l) affects the phase velocity more than the nonlocal parameter (μ).
- Increasing ΔT in UTR and HC thermal loadings leads to a decrease in the phase velocities, especially for $\zeta\leq1$. Longitudinal and flexural waves are more affected than shear waves. In general, the effect of UTR thermal loading on phase velocity is more remarkable than HC thermal loading.
- An Increase in the arc angle causes the phase velocity to experience more variations concerning the wavenumber changes. The lower the L/h ratio, the more visible this behavior. In this regard, the phase velocity of the longitudinal wave is more affected than in other cases.
- An increase in ceramic percentage in the FG curved nanobeam material (decreasing the k) leads to the emergence of the stiffness-hardening effects. As a result, the phase velocity increases, becoming more sensitive to the wavenumber variations.

These results can be helpful in future studies of wave propagation in curved nanostructures. Also, these can give better insights to researchers about how to design nano-devices.

Acknowledgment

This research did not receive any specific grant from funding agencies in the public, commercial, or not-for-profit sectors.

References

Akgöz, B. and Ö. Civalek (2013), "Longitudinal vibration analysis of strain gradient bars made of functionally graded materials (FGM)", *Compos. Part B Eng.*, **55**, 263-268. https://doi.org/10.1016/j.compositesb.2013.06.035.

Al-Furjan, M., M.A. Oyarhossein, M. Habibi, H. Safarpour, D.W. Jung and A. Tounsi (2021), "On the wave propagation of the multi-scale hybrid nanocomposite doubly curved viscoelastic panel", *Compos. Struct.*, **255**, 112947. https://doi.org/10.1016/j.compstruct.2020.112947.

Alazwari, M.A., I. Esen, A.A. Abdelrahman, A.M. Abdraboh and M.A. Eltaher (2022), "Dynamic analysis of functionally graded (FG) nonlocal strain gradient nanobeams under thermo-magnetic fields and moving load", *Adv. Nano Res.*, **12**(3), 231-251. https://doi.org/10.12989/anr.2022.12.3.231.

Alwabli, A.S., A. Kaci, H. Bellifa, A.A. Bousahla, A. Tounsi, D.A. Alzahrani, A.A. Abulfaraj, F. Bourada, K.H. Benrahou and A. Tounsi (2021), "The nano scale buckling properties of isolated protein microtubules based on modified strain gradient theory and a new single variable trigonometric beam theory", *Adv. Nano Res.*, **10**(1), 15-24. https://doi.org/10.12989/anr.2021.10.1.015.

Arefi, M. and A.M. Zenkour (2017), "Wave propagation analysis of a functionally graded magneto-electro-elastic nanobeam rest on Visco-Pasternak foundation", *Mech. Res. Commun.*, **79**, 51-62. https://doi.org/10.1016/j.mechrescom.2017.01.004.

Attia, M.A. (2017), "On the mechanics of functionally graded nanobeams with the account of surface elasticity", *Int. Eng. Sci.*, **115**, 73-101. https://doi.org/10.1016/j.ijengsci.2017.03.011.

Barretta, R., F.M. de Sciarra and M.S. Vaccaro (2019), "On nonlocal mechanics of curved elastic beams", *Int. Eng. Sci.*, **144**, 103140. https://doi.org/10.1016/j.ijengsci.2019.103140.

Bensaid, I., A. Bekhadda and B. Kerboua (2018), "Dynamic analysis of higher order shear-deformable nanobeams resting on elastic foundation based on nonlocal strain gradient theory", *Adv. Nano Res.*, **6**(3), 279. https://doi.org/10.12989/anr.2018.6.3.279.

Boyina, K. and R. Piska (2023), "Wave propagation analysis in viscoelastic Timoshenko nanobeams under surface and magnetic field effects based on nonlocal strain gradient theory", *Appl. Math. Comput.*, **439**, 127580. https://doi.org/10.1016/j.amc.2022.127580.

Carbonari, R.C., E.C. Silva and G.H. Paulino (2009), "Multi-actuated functionally graded piezoelectric micro-tools design: A multiphysics topology optimization approach", *Int. J. Numer. Meth. Eng.*, **77**(3), 301-336. https://doi.org/10.1002/nme.2403.

Ebrahimi, F., A. Dabbagh, T. Rabczuk and F. Tornabene (2019a), "Analysis of propagation characteristics of elastic waves in heterogeneous nanobeams employing a new two-step porosity-dependent homogenization scheme", *Adv. Nano Res.*, **7**(2), 135. https://doi.org/10.12989/anr.2019.7.2.135.

Ebrahimi, F., A. Seyfi and A. Dabbagh (2019b), "Dispersion of waves in FG porous nanoscale plates based on NSGT in thermal environment", *Adv. Nano Res.*, **7**(5), 325-335. https://doi.org/10.12989/anr.2019.7.5.325.

Eltaher, M., M. Khater and S.A. Emam (2016), "A review on nonlocal elastic models for bending, buckling, vibrations, and wave propagation of nanoscale beams", *Appl. Math. Modell.*, **40**, 5-6, 4109-4128. https://doi.org/10.1016/j.apm.2015.11.026.

Eringen, A.C. (1983), "On differential equations of nonlocal elasticity and solutions of screw dislocation and surface waves", *J. Appl. Phys.*, **54**(9), 4703-4710. https://doi.org/10.1063/1.332803.

Faroughi, S., A. Rahmani and M. Friswell (2020), "On wave propagation in two-dimensional functionally graded porous rotating nano-beams using a general nonlocal higher-order beam model", *Appl. Math. Modell.*, **80**, 169-190. https://doi.org/10.1016/j.apm.2019.11.040.

Ganapathi, M. and O. Polit (2018), "A nonlocal higher-order model including thickness stretching effect for bending and buckling of curved nanobeams", *Appl. Math. Modell.*, **57**, 121-141. https://doi.org/10.1016/j.apm.2017.12.025.

Ghandourah, E.E., H.M. Ahmed, M.A. Eltaher, M.A. Attia and A.M. Abdraboh (2021), "Free vibration of porous FG nonlocal modified couple nanobeams via a modified porosity model", *Adv. Nano Res.*, **11**(4), 405-422. https://doi.org/10.12989/anr.2021.11.4.405.

Ghayesh, M.H. and A. Farajpour (2019), "A review on the mechanics of functionally graded nanoscale and microscale structures", *Int. Eng. Sci.*, **137**, 8-36. https://doi.org/10.1016/j.ijengsci.2018.12.001.

Gorgani, H.H., M.M. Adeli and M. Hosseini (2019), "Pull-in behavior of functionally graded micro/nano-beams for MEMS and NEMS switches", *Microsyst. Technol.*, **25**(8), 3165-3173. https://doi.org/10.1007/s00542-018-4216-4.

Hadji, L. and M. Avcar (2021), "Nonlocal free vibration analysis of porous FG nanobeams using hyperbolic shear deformation beam theory", *Adv. Nano Res.*, **10**(3), 281-293. https://doi.org/10.12989/anr.2021.10.3.281.

Hashemian, A. and S.F. Hosseini (2019), "Nonlinear bifurcation analysis of statically loaded free-form curved beams using isogeometric framework and pseudo-arclength continuation", *Int. J. Non-Linear Mech.*, **113**, 1-16. https://doi.org/10.1016/j.ijnonlinmec.2019.03.002.

Hu, T., W. Yang, X. Liang and S. Shen (2018), "Wave propagation in flexoelectric microstructured solids", *J. Elast.*, **130**, 2, 197-210. https://doi.org/10.1007/s10659-017-9636-3.

Kiani, K. (2016), "Thermo-elasto-dynamic analysis of axially functionally graded non-uniform nanobeams with surface energy", *Int. Eng. Sci.*, **106**, 57-76. https://doi.org/10.1016/j.ijengsci.2016.05.004.

Kiani, Y., M. Rezaei, S. Taheri and M. Eslami (2011), "Thermo-electrical buckling of piezoelectric functionally graded material Timoshenko beams", *Int. J. Mech. Mater. Des.*, **7**(3), 185-197. https://doi.org/10.1007/s10999-011-9158-2.

Komeili, A., A.H. Akbarzadeh, A. Doroushi and M.R. Eslami (2011), "Static analysis of functionally graded piezoelectric beams under thermo-electro-mechanical loads", *Adv. Mech. Eng.*, **3**, 153731. https://doi.org/10.1155/2011/153731.

Komijani, M., S. Esfahani, J. Reddy, Y. Liu and M. Eslami (2014), "Nonlinear thermal stability and vibration of pre/post-buckled temperature-and microstructure-dependent functionally graded beams resting on elastic foundation", *Compos. Struct.*, **112**, 292-307. https://doi.org/10.1016/j.compstruct.2014.01.041.

Komijani, M., Y. Kiani, S. Esfahani and M. Eslami (2013), "Vibration of thermo-electrically post-buckled rectangular functionally graded piezoelectric beams", *Compos. Struct.*, **98**,

143-152. https://doi.org/10.1016/j.compstruct.2012.10.047.
Lai, W.M., D.H. Rubin, D. Rubin and E. Krempl (2009), *Introduction to Continuum Mechanics*, Butterworth-Heinemann.
Lam, D.C., F. Yang, A. Chong, J. Wang and P. Tong (2003), "Experiments and theory in strain gradient elasticity", *J. Mech. Phys. Solids*, **51**(8), 1477-1508. https://doi.org/10.1016/S0022-5096(03)00053-X.
Li, C., C. Zhu, N. Zhang, S. Sui and J. Zhao (2022), "Free vibration of self-powered nanoribbons subjected to thermal-mechanical-electrical fields based on a nonlocal strain gradient theory", *Appl. Math. Modell.*, **110**, 583-602. https://doi.org/10.1016/j.apm.2022.05.044,
Li, L., Y. Hu and L. Ling (2015), "Flexural wave propagation in small-scaled functionally graded beams via a nonlocal strain gradient theory", *Compos. Struct.*, **133**, 1079-1092. https://doi.org/10.1016/j.compstruct.2015.08.014.
Lim, C., G. Zhang and J. Reddy (2015), "A higher-order nonlocal elasticity and strain gradient theory and its applications in wave propagation", *J. Mech. Phys. Solids*, **78**, 298-313. https://doi.org/10.1016/j.jmps.2015.02.001.
Liu, Y. and J. Reddy (2011), "A nonlocal curved beam model based on a modified couple stress theory", *Int. J. Struct. Stabil. Dyn.*, **11**(3), 495-512. https://doi.org/10.1142/S0219455411004233.
Lu, L., X. Guo and J. Zhao (2017), "Size-dependent vibration analysis of nanobeams based on the nonlocal strain gradient theory", *Int. Eng. Sci.*, **116**, 12-24. https://doi.org/10.1016/j.ijengsci.2017.03.006.
Ma, L.H., L.L. Ke, Y.Z. Wang and Y.S. Wang (2017), "Wave propagation in magneto-electro-elastic nanobeams via two nonlocal beam models", *Physica E*, **86**, 253-261. https://doi.org/10.1016/j.physe.2016.10.036.
Matouk, H., A.A. Bousahla, H. Heireche, F. Bourada, E. Bedia, A. Tounsi, S. Mahmoud, A. Tounsi and K. Benrahou (2020), "Investigation on hygro-thermal vibration of P-FG and symmetric S-FG nanobeam using integral Timoshenko beam theory", *Adv. Nano Res.*, **8**(4), 293-305. https://doi.org/10.12989/anr.2020.8.4.293.
Miller, R.E. and V.B. Shenoy (2000), "Size-dependent elastic properties of nanosized structural elements", *Nanotechnology*, **11**(3), 139. http://doi.org/10.1088/0957-4484/11/3/301.
Mindlin, R.D. (1965), "Second gradient of strain and surface-tension in linear elasticity", *Int. J. Solids Struct.*, **1**(4), 417-438. https://doi.org/10.1016/0020-7683(65)90006-5.
Mohammadimehr, M., M. Farahi and S. Alimirzaei (2016), "Vibration and wave propagation analysis of twisted micro-beam using strain gradient theory", *Appl. Math. Mech.*, **37**(10), 1375-1392. https://doi.org/10.1007/s10483-016-2138-9.
Nanda, N. and S. Kapuria (2015), "Spectral finite element for wave propagation analysis of laminated composite curved beams using classical and first order shear deformation theories", *Compos. Struct.*, **132**, 310-320. https://doi.org/10.1016/j.compstruct.2015.04.061.
Numanoğlu, H.M. and Ö. Civalek (2019), "On the dynamics of small-sized structures", *Int. Eng. Sci.*, **145**, 103164. https://doi.org/10.1016/j.ijengsci.2019.103164.
Papargyri-Beskou, S., D. Polyzos and D. Beskos (2009), "Wave dispersion in gradient elastic solids and structures: a unified treatment", *Int. J. Solids Struct.*, **46**(21), 3751-3759. https://doi.org/10.1016/j.ijsolstr.2009.05.002.
Rahaeifard, M., M. Kahrobaiyan and M. Ahmadian (2010), "Sensitivity analysis of atomic force microscope cantilever made of functionally graded materials", *Proceedings of the ASME 2009 International Design Engineering Technical Conferences and Computers And Information In Engineering Conference, American Society of Mechanical Engineers Digital Collection*. https://doi.org/10.1115/DETC2009-86254.
Rahmani, O., S. Hosseini, I. Ghoytasi and H. Golmohammadi (2017), "Buckling and free vibration of shallow curved micro/nano-beam based on strain gradient theory under thermal loading with temperature-dependent properties", *Appl. Phys. A*, **123**(1), 4. https://doi.org/10.1007/s00339-016-0591-9.
Rahmani, O., S. Hosseini, I. Ghoytasi and H. Golmohammadi (2018), "Free vibration of deep curved FG nano-beam based on modified couple stress theory", *Steel Compos. Struct.*, **26**(5), 607-620. https://doi.org/10.12989/scs.2018.26.5.607.
Reddy, J. and C. Chin (1998), "Thermomechanical analysis of functionally graded cylinders and plates", *J. Therm. Stress.*, **21**(6), 593-626. https://doi.org/10.1080/01495739808956165.
Sadeghi, H., M. Baghani and R. Naghdabadi (2012), "Strain gradient elasticity solution for functionally graded micro-cylinders", *Int. Eng. Sci.*, **50**(1), 22-30. https://doi.org/10.1016/j.ijengsci.2011.09.006.
Shabana, Y.M., M.A. Samy, M.A. Abdel-Aziz, M.E. Hindawi, M.G. Mosry, A.R.M. Albarawy, M.M. Omar, A.A. Mohamed and A.A. Attia (2021), "Enhancing the performance of micro-biosensors by functionally graded geometrical and material parameters", *Arch. Appl. Mech.*, **91**(6), 2497-2511. https://doi.org/10.1007/s00419-021-01900-w.
Shahsavari, D., B. Karami and A. Tounsi (2023), "Wave propagation in a porous functionally graded curved viscoelastic nano-size beam", *Wave Random Complex Med.*, **1-22**. https://doi.org/10.1080/17455030.2022.2164376.
She, G.L., F.G. Yuan and Y.R. Ren (2018), "On wave propagation of porous nanotubes", *Int. Eng. Sci.*, **130**, 62-74. https://doi.org/10.1016/j.ijengsci.2018.05.002.
Shen, H.S. (2016), *Functionally graded materials: nonlinear analysis of plates and shells*, CRC press.
Şimşek, M. (2019), "Some closed-form solutions for static, buckling, free and forced vibration of functionally graded (FG) nanobeams using nonlocal strain gradient theory", *Compos. Struct.*, **224**, 111041. https://doi.org/10.1016/j.compstruct.2019.111041.
Timoshenko, S. P. (1922), "X. On the transverse vibrations of bars of uniform cross-section", *The London, Edinburgh, and Dublin Philosophical Magazine and Journal of Science*, **43**, 253, 125-131. https://doi.org/10.1080/14786442208633855.
Tlidji, Y., R. Benferhat, T.H. Daouadji, A. Tounsi and L.C. Trinh (2022), "Free vibration analysis of FGP nanobeams with classical and non-classical boundary conditions using State-space approach", *Adv. Nano Res.*, **13**(5), 453-463. https://doi.org/10.12989/anr.2022.13.5.453.
Wang, X., X. Ren, H. Zhou, J. Yu and K. Li (2023), "Dynamics of thermoelastic Lamb waves in functionally graded nanoplates based on the modified nonlocal theory", *Appl. Math. Modell.*, **117**, 142-161. https://doi.org/10.1016/j.apm.2022.12.022.
Xing, L., W. Liu, X. Li, H. Wang, Z. Jiang and L. Wang (2022), "Application of machine learning and deep neural network for wave propagation in lung cancer cell", *Adv. Nano Res.*, **13**(3), 297-312. https://doi.org/10.12989/anr.2022.13.3.297.
Xu, F., Q. Qin, A. Mishra, Y. Gu and Y. Zhu (2010), "Mechanical properties of ZnO nanowires under different loading modes", *Nano Res.*, **3**(4), 271-280. https://doi.org/10.1007/s12274-010-1030-4.
Yan, Z. and L. Jiang (2011), "Electromechanical response of a curved piezoelectric nanobeam with the consideration of surface effects", *J. Phys. D Appl. Phys.*, **44**(36), 365301. http://doi.org/10.1088/0022- 3727/44/36/365301.
Yang, F., A. Chong, D.C.C. Lam and P. Tong (2002), "Couple stress based strain gradient theory for elasticity", *Int. J. Solids Struct.*, **39**(10), 2731-2743. https://doi.org/10.1016/S0020-7683(02)00152-X.
Zenkour, A.M. and M. Sobhy (2015), "A simplified shear and normal deformations nonlocal theory for bending of nanobeams

in thermal environment", *Physica E*, **70**, 121-128. https://doi.org/10.1016/j.physe.2015.02.022.
Zhao, J. and Z. Yu (2021), "On the modeling and simulation of the nonlinear dynamic response of NEMS via a couple of nonlocal strain gradient theory and classical beam theory", *Adv. Nano Res.*, **11**(5), 547. https://doi.org/10.12989/anr.2021.11.5.547.

CC